

Real-time monitoring of nanoparticle retention in porous media

Jeff Rottman · Reyes Sierra-Alvarez ·
Farhang Shadman

Received: 23 April 2012 / Accepted: 7 September 2012 / Published online: 16 September 2012
© Springer-Verlag 2012

Abstract Nanoparticles are not specifically targeted in conventional treatment schemes; consequently, typical wastewater treatment systems are ineffective for nanoparticles removal. With rapidly increasing concern over their health effects, improved understanding of nanoparticle transport and retention in porous media filters is critical because of its application in new wastewater treatment methods and for assessment of the fate of the discharged nanoparticles in soil. In this study, a unique and robust integrated method is developed and validated. Experimentally, this approach uses an on-line, real-time, and in situ method for measuring nanoparticle retention dynamics, eliminating the laborious and less accurate sampling and off-line analysis. The data analysis part is a process simulator which provides both kinetic properties of the retention process as well as the overall capacity and loading. This technique is validated by application to the transport and retention of TiO₂ nanoparticles in two vastly different porous filtration media—activated carbon and sand. TiO₂ retained concentrations ranged from 0.24 to 0.37 mg g⁻¹ for activated carbon and 0.01–0.014 mg g⁻¹ for sand. The integrated method presented here is useful for both comparison of the filtration effectiveness of various porous materials as well as for process optimization and scale-up for industrial applications.

Keywords Activated carbon · Dispersant · Model · Nanomaterials · Sand · TiO₂

Introduction

The use of nanoparticles in manufacturing continues to increase (US EPA 2007), raising concerns over their environmental and health effects (Auffan et al. 2009; Handy and Shaw 2007). Inorganic oxide nanoparticles, in particular, have growing applications in catalysis, polymers, coatings, etc. A large amount of these nanoparticles are contained in wastewater streams (Boxall et al. 2007). Released nanoparticles can be exposed to porous media through water treatment techniques, such as slow or rapid sand filtration, or during transport through soil or sediments. Understanding transport and removal mechanisms in porous media is of utmost importance to develop treatment technologies specifically designed for the removal of nanomaterials as well as to determine environmental fate.

The transport, deposition, and retention of nanoparticles in saturated porous media have been examined recently (Ben-Moshe et al. 2010; Chen et al. 2011; Godinez and Darnault 2011; Solovitch et al. 2010). Nanoparticle behavior is highly influenced by solution chemistry, such as pH, ionic strength, and valence and concentration of ionic species (Dunphy Guzman et al. 2006; French et al. 2009). Mechanistic studies have shown that electrical double layer interactions strongly influence retention of inorganic oxide nanoparticles. With the significant variance of influencing factors, a fast, simple, accurate technique for the measurement of nanoparticle retention in porous media would be highly profitable.

The most common techniques for measuring the concentration of nanoparticles in porous media filtration experiments are UV–Vis spectrophotometry (Kim et al. 2009; Lecoanet et al. 2004; Lecoanet and Wiesner 2004) or inductively coupled plasma atomic emission spectroscopy (ICP-AES) analysis of acid-digested samples (Ben-Moshe

J. Rottman (✉) · R. Sierra-Alvarez · F. Shadman
Department of Chemical and Environmental Engineering,
University of Arizona, P.O. Box 210011, Tucson,
AZ 85721, USA
e-mail: jrottman@email.arizona.edu

et al. 2010; Solovitch et al. 2010). Common problems associated with both of these techniques are sample collection as well as time-consuming preparation, and analysis procedures. Sampling provides opportunities for error in mass balance, especially in the case of ICP-AES measurement, as a digestion step is often necessary prior to analysis. Measurement delay could also result in the aggregation or settling of nanoparticles which could interfere with UV-Vis measurements. Finally, sampling adds unnecessary complexity to the experiment and digestion, and ICP-AES analysis is laborious and more costly. To determine dynamics by sampling, a large amount of samples must be taken over a short time; online measurement is advantageous due to its simplicity and improved accuracy.

In this work, an approach to monitoring nanoparticle retention in porous media utilizing online UV-Vis absorbance measurements is demonstrated. Additionally, a basic transport model describing both physical and chemical nanoparticle-media interactions is set forth. Application of this model, along with the ability to rapidly obtain data on nanoparticle transport under various conditions using the proposed apparatus, provides a basis for developing more effective strategies for the treatment of effluents containing nanoparticles.

Experimental

Materials

Nano-TiO₂ (Aeroxide P25, 25 nm) was obtained from Evonik Industries (Essen, Germany). Two types of porous media were used, sand and granular activated carbon (GAC). The quartz sand (Acros Organics, Geel, Belgium) had a size range of 149–400 μm and were washed prior to use with 10 % HNO₃, rinsed with deionized water and dried at 105 °C. The GAC (KCI-40 AD, KC International, Thousand Palms, CA, USA) ranged in particle size from 400 to 1,680 μm. The GAC was rinsed thoroughly with deionized water under ultrasonic agitation to remove fines and then saturated with deionized water prior to column packing.

TiO₂ suspensions (50 mg L⁻¹) were prepared in a phosphate buffer (0.5 mM, pH 7, 1 mM ionic strength). Dispersions were sonicated before the start of an experiment using a Cole-Parmer ultrasonic processor (Vernon Hills, IL, USA) at 65 % intensity for 5 min.

Experimental setup

Figure 1 shows a framework of the experimental apparatus. The glass column (diameter = 15 mm, length = 150 mm, Omnifit Benchmark, Diba Industries, Danbury, CT, USA)

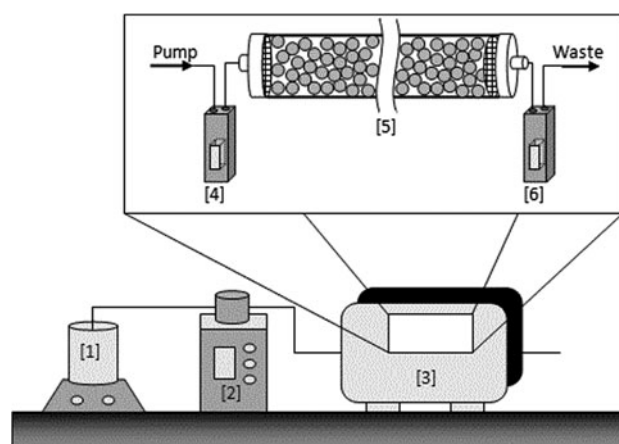


Fig. 1 Online experimental apparatus including continuously stirred nanoparticle suspension [1] peristaltic pump [2], UV-Vis spectrophotometer [3], flow-through cuvettes for influent [4] and effluent [6], and glass particle packed with porous media [5]. This apparatus provides fully online data of nanoparticle retention in the column without the need for sampling or further sample preparation prior to measurement

was connected to flow-through quartz cuvettes (10 mm path length, Starna Cells Inc., Atascadero, CA, USA) using PTFE tubing. The nanoparticle dispersion was fed using a Micropuls3 peristaltic pump (Gilson Inc., Middleton, WI, USA). Absorbance at 300 nm was monitored for the inlet and outlet of the column at 10-s intervals using a UV-Vis spectrophotometer (UV 1800, Shimadzu Corporation, Kyoto, Japan).

Column preparation varied slightly between sand and activated carbon. Sand columns were dry packed with 36.5 g of sand under agitation from an ultrasonic bath. The sand column was then filled from the bottom with deionized water to ensure wetting of the bed and facilitate removal of trapped air. GAC columns were wet packed with 10.5 g (dry weight) GAC. The columns were then rinsed with deionized water in an ultrasonic bath to ensure elution of any remaining fines. Column porosity was determined by measuring the entrained water mass after rinsing. A phosphate buffer (0.5 mM, pH 7, 1 mM ionic strength) was prepared, and ammonium polyacrylate dispersant (Dispex A40, BASF Chemical Co., Freeport, TX, USA), if used, was added at 0.1 g L⁻¹ prior to final pH adjustment. A portion of this solution was then separated to prerinse the column, displacing 5 bed volumes, so that the pore solution in the column was identical to that used in the nanoparticle suspension.

The nanoparticle suspension was pumped through the column at a rate of 2.6 mL min⁻¹ for 30 bed volumes. Inlet and outlet dispersion samples were collected at 10 bed volume intervals and tested for size distribution and zeta potential as well as titanium content. Post run, the column was rinsed for 5 bed volumes with the NP-free background

solution. Samples of the column media were then taken at five locations equidistant throughout the column set aside for titanium analysis in order to determine the media-associated nanoparticle concentration. All experiments were performed in triplicate.

Analysis

TiO₂ NPs were imaged by transmission electron microscope (TEM) using a Hitachi H8100 (Hitachi High-Technologies Corp., Tokyo, Japan) at 200 keV. The zeta potential of nanoparticle dispersions was measured immediately after sampling by a ZetaSizer Nano ZS (Malvern, Inc., Sirouthborough, MA, USA) using laser Doppler velocimetry. Particle size distribution measurements were conducted by dynamic light scattering using the same instrument. Elemental analysis of the samples for titanium content was performed in two steps. First, the samples were digested with equal parts HNO₃ (70 %) and H₂SO₄ (95 %) in a microwave-assisted extraction system (120 °C, 45 min, MARS Xpress, CEM Corp, Matthews, NC, USA). The samples were then diluted and analyzed by ICP-AES (334.94 nm, Optima 2100DV, Perkin Elmer, Waltham, MA, USA).

Results and discussion

TiO₂ nanoparticles

TiO₂ nanoparticle size distributions were obtained in the buffer solution with and without added dispersant. The average particle sizes came to 194 and 200 nm, respectively, as shown in Fig. 2. Also shown in Fig. 2, the nanoparticle morphology, determined by TEM imaging, is nearly spherical and crystalline.

Apparatus performance

The proposed technique allows rapid, simultaneous measurement of the nanoparticle concentration in both the influent and effluent of the column by utilizing flow-through cuvettes in the reference and measurement cells of a UV–Vis spectrophotometer. The absorption difference between the cells is constantly measured, resulting in detailed breakthrough curves, as shown in Fig. 3a for nanoparticles in columns packed with clean sand or GAC. Negative values in the first bed volume are within the range of error of zero and are artifacts of the calibration curve. This calibration line ($C_{NP} = 20.08 \cdot A_b + 0.64$, $R^2 = 0.999$) provides an applicable range from 1 to 60 mg TiO₂ L⁻¹. The small standard deviation of the triplicate measurements emphasizes the high reproducibility and precision of the technique.

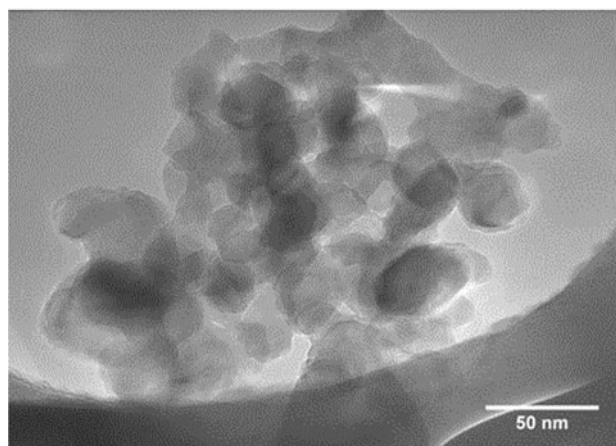
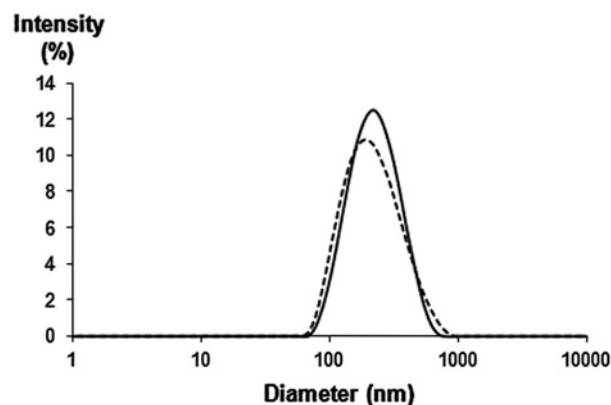


Fig. 2 Particle size distribution (*top*) of the TiO₂ nanoparticle dispersion with no additive (*line*) and with synthetic dispersant, Dispex (*dotted line*) which provide average particle sizes of 200 and 190 nm, respectively. The transmission electron microscopy image (*below*) of the TiO₂ nanoparticles displays their spherical and crystalline structure

Sand showed a very poor affinity for the nanoparticles, and breakthrough was observed in just over two bed volumes. This is likely due to large electrostatic repulsion between the similarly charged nanoparticles and sand, as noted with early breakthrough elsewhere (Chen et al. 2011; Solovitch et al. 2010). Activated carbon, alternatively, showed a higher affinity for nano-TiO₂. After an initial rise to approximately 60 % influent concentration, a much slower retention mechanism became dominant. This increased capture is possibly due to the ability of nanoparticles to diffuse into the complex pore network of GAC; however, this hypothesis would require further investigation. Currently, there are no published studies considering the use of activated carbon as an adsorptive media for nanoparticles.

The addition of a dispersant, Dispex A40, effectively stabilized the nanoparticles through increasing the negative charge density on the surface and led to rapid nanoparticle breakthrough both in sand- and GAC-packed columns (Fig. 3b). The zeta potential of the TiO₂ dispersions

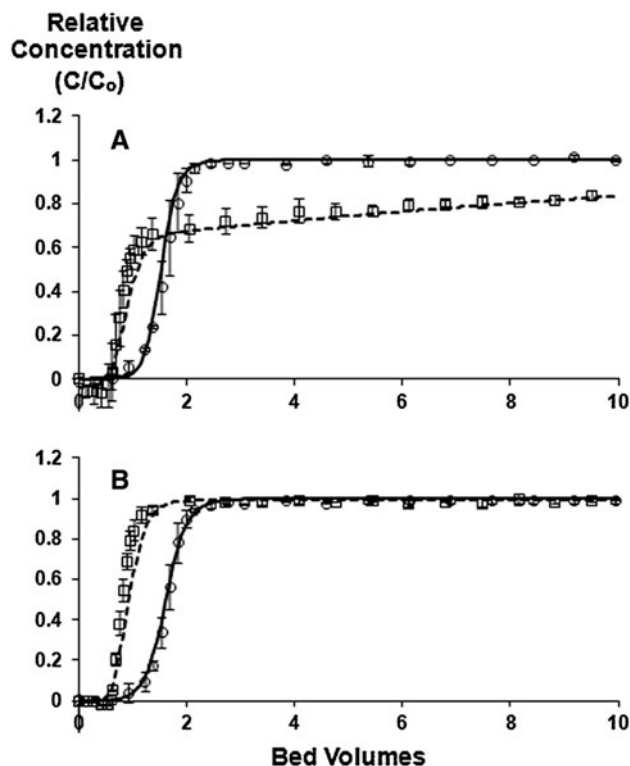


Fig. 3 Breakthrough curves of TiO₂ NPs with no additives (a) and with the presence of synthetic dispersant Dispex (b) in beds packed with sand (circle) and activated carbon (rectangle) along with the best-fit model results shown for sand (solid line) and activated carbon (dotted line). Error bars indicate standard deviation for three runs. Both show versatility and accuracy of the online measurement technique. In (a), note the rapid breakthrough for the sand bed versus the greater affinity shown in the slow approach to breakthrough for activated carbon. The model not only captures the simple breakthrough curve for sand, but also the more complicated dual regimes of activated carbon. Dispex is highly effective at stabilizing the nanoparticle as shown by the rapid breakthrough of TiO₂ for both media (b)

supplied with Dispex decreased to -52 mV, thus further diminishing the association of the nanoparticles with sand. With GAC, the increased electrostatic repulsion between the nanoparticles likely hindered their migration into more constricted pore space. The hydrophilic dispersant may have also contributed to reduce nanoparticle affinity for the hydrophobic GAC. The negative impact of synthetic dispersants on NP retention by porous media has been reported (Jeong and Kim 2009; Lin et al. 2010; Tian et al. 2010). This result displays the sensitivity of nanoparticle retention resulting from a change in solution characteristics and the ability of the technique to monitor this change in highly unfavorable sorption conditions.

Overall, it is shown that the online measurement of nanoparticle retention is highly sensitive, allowing for detailed contours of the breakthrough curve, as well as rapid and highly repeatable, as evidenced by the low standard

deviations between replicates. While measurement by UV absorbance has pitfalls and limitations, such as interference from UV-absorbing compounds, this technique prevents against sampling error, provides a large number of points at small intervals nearing continuous monitoring, and provides the real-time in situ measurement required for the intended application as a method of “process control” in treatment systems. This produces a pathway to better understanding of the influence both media and solution characteristics have on nanoparticle retention. Modeling of this interaction should further aid in clarifying the dominant mechanisms.

Modeling

Developing a process model of nanoparticle behavior in porous media is an important part of the proposed methodology as it facilitates parametric study, process optimization, and ultimately allows the study to be scaled up to industrial applications. The model was developed based on first-order attachment/detachment. This model, Eqs. (1) and (2), includes the time (t) and bed-length dimension (z) dependence of both nanoparticle concentration in the liquid phase, C (g m^{-3}), and nanoparticle concentration on the surface, C_s (g m^{-2}). Here, D ($\text{m}^2 \text{s}^{-1}$) is the coefficient of dispersion, U (m s^{-1}) is the interstitial liquid velocity, r (m) is the average radius of the bed media, ε is the bed porosity, θ is the fractional surface coverage ($C_s/C_{s,max}$), and k_a ($\text{m}^3 \text{m}^{-2} \text{s}^{-1}$) and k_d ($\text{g m}^{-2} \text{s}^{-1}$) are first-order attachment and detachment rate coefficients.

$$\frac{\partial C}{\partial t} = D \frac{\partial^2 C}{\partial z^2} - U \frac{\partial C}{\partial z} - \frac{3(1-\varepsilon)}{r\varepsilon} \frac{\partial C_s}{\partial t} \quad (1)$$

$$\frac{\partial C_s}{\partial t} = k_a C(1-\theta) - k_d \theta \quad (2)$$

Fitting the curves was accomplished by adjusting three parameters: D , k_a , and k_d . An initial estimate of dispersion was implemented utilizing an equation developed by Singh (Singh 1998) for ideal solutes in soil columns. Additionally, $C_{s,max}$ was estimated using previously calculated capacity data for the nanoparticles under the tested conditions: 3.0×10^{-4} and 0.065 g m^{-2} for sand and GAC, respectively. For the entirety of this modeling work, k_d was set to zero, as no evidence for detachment was observed. It should be noted that the curve analysis utilizes the data from the section of the curve just after the start of breakthrough and before full bed exhaustion, as the data prior to this point provide information on the capacity, not the dynamics of the changing bed which is desired.

Nanoparticle breakthrough curves for both sand and GAC are compared with model results in Fig. 3. The transport of TiO₂ in the sand bed seems to be primarily controlled by dispersion as expected due to the large electrostatic repulsion

which limits attachment. In the case of GAC, however, two regimes were evident: the rapid initial effluence dominated by dispersion and the slower approach to full breakthrough dominated by adsorption. Both mechanisms are captured by the proposed model. The differences in dispersion between the two beds, 1.0×10^{-5} and $3.0 \times 10^{-6} \text{ m}^2 \text{ s}^{-1}$ for sand and GAC, respectively, are attributable to the significant change in porosity, from 0.214 for sand to 0.482 for GAC. It is interesting to note that the attachment rate coefficient (k_a) determined for GAC ($5.0 \times 10^{-7} \text{ m}^3 \text{ m}^{-2} \text{ s}^{-1}$) is half that of sand ($1.0 \times 10^{-6} \text{ m}^3 \text{ m}^{-2} \text{ s}^{-1}$). This is likely a result of the nature of these rate constants, as they encompass all mechanisms corresponding to attachment, the slower diffusion into the GAC pores could explain the discrepancy. Overall, model predictions had a relatively high degree of accuracy, with R^2 values of 0.99 for sand and 0.94 for GAC. Expansion of the rate constants will elucidate controlling parameters and allow for more effective design of treatment technologies.

The model also provides information on the concentration of nanoparticles retained as a function of bed length. Comparisons of TiO_2 bed concentrations with the model predictions are shown in Fig. 4. The experimental data indicate that TiO_2 retention by GAC, 0.24–0.37 mg g^{-1} GAC, was over one order of magnitude greater than sand, 0.01–0.014 mg g^{-1} . The model, fit primarily to the breakthrough curve, produced a relatively accurate prediction of the captured nanoparticle concentration. The prediction of the associated nanoparticle bed profile allows for better estimation of effective bed lifetime.

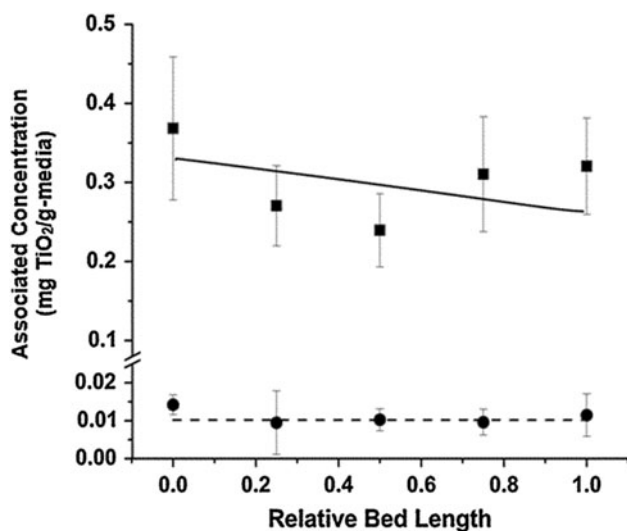


Fig. 4 Concentration of TiO_2 nanoparticles retained by sand (filled circle), activated carbon (filled square), along with best fit model results shown for sand (solid line) and activated carbon (dotted line). Evident is the significantly higher retained concentration of TiO_2 on activated carbon as compared to sand. Also, the model gives an accurate description of these measurements. Retained concentration profiles are important in predicting potential for industrial scale-up

Conclusion

The method developed and validated in this study provides a rapid, robust approach for monitoring nanoparticle retention in porous media. The major advantage and uniqueness of this method is in using an on-line, real-time, and in situ method for measuring nanoparticle transport and retention dynamics; this eliminates the complexity and errors of sampling and off-line analysis. The method was applied and tested for TiO_2 nanoparticles in two porous filtration media, GAC and sand, which provided retained concentrations of 0.24–0.37 mg g^{-1} and 0.01–0.014 mg g^{-1} , respectively. The experimental approach is integrated with a process simulator which provides both kinetic properties of the process as well as the breakthrough and capacity. The method is useful for determining the role of various transport mechanisms, process bottlenecks, and values of fundamental process parameters. The model's ability to translate the small-system data into these fundamental parameters informs scale-up, design, and operational parametric study of large systems under various conditions.

Acknowledgments We would like to thank SRC/Sematech Engineering Research Center for funding this work. J. Rottman was supported by a graduate fellowship from the Intel Foundation.

References

- Auffan M, Rose J, Bottero JY et al (2009) Towards a definition of inorganic nanoparticles from an environmental, health and safety perspective. *Nat Nanotechnol* 10:634–641
- Ben-Moshe T, Dror I, Berkowitz B (2010) Transport of metal oxide nanoparticles in saturated porous media. *Chemosphere* 3: 387–393
- Boxall AB, Tiede K, Chaudhry Q (2007) Engineered nanomaterials in soils and water: how do they behave and could they pose a risk to human health? *Nanomedicine* 6:919–927
- Chen GX, Liu XY, Su CM (2011) Transport and retention of TiO_2 rutile nanoparticles in saturated porous media under low-ionic-strength conditions: measurements and mechanisms. *Langmuir* 9:5393–5402
- Dunphy Guzman KA, Finnegan MP, Banfield JF (2006) Influence of surface potential on aggregation and transport of titania nanoparticles. *Environ Sci Technol* 24:7688–7693
- French RA, Jacobson AR, Kim B et al (2009) Influence of ionic strength, pH, and cation valence on aggregation kinetics of titanium dioxide nanoparticles. *Environ Sci Technol* 5: 1354–1359
- Godinez IG, Darnault CJG (2011) Aggregation and transport of nano- TiO_2 in saturated porous media: effects of pH, surfactants and flow velocity. *Water Res* 2:839–851
- Handy RD, Shaw BJ (2007) Toxic effects of nanoparticles and nanomaterials: implications for public health, risk assessment and the public perception of nanotechnology. *Health Risk Soc* 2: 125–144
- Jeong SW, Kim SD (2009) Aggregation and transport of copper oxide nanoparticles in porous media. *J Environ Monit* 9:1595–1600

- Kim HJ, Phenrat T, Tilton RD et al (2009) Fe-0 nanoparticles remain mobile in porous media after aging due to slow desorption of polymeric surface modifiers. *Environ Sci Technol* 10:3824–3830
- Lecoanet HF, Wiesner MR (2004) Velocity effects on fullerene and oxide nanoparticle deposition in porous media. *Environ Sci Technol* 16:4377–4382
- Lecoanet HF, Bottero JY, Wiesner MR (2004) Laboratory assessment of the mobility of nanomaterials in porous media. *Environ Sci Technol* 19:5164–5169
- Lin DH, Tian XL, Wu FC et al (2010) Fate and transport of engineered nanomaterials in the environment. *J Environ Qual* 6: 1896–1908
- Singh SK (1998) Estimation of dispersion coefficient from data on soil column test. IX National Symposium on Hydrology, Amritsar
- Solovitch N, Labille J, Rose J et al (2010) Concurrent aggregation and deposition of TiO₂ nanoparticles in a sandy porous media. *Environ Sci Technol* 13:4897–4902
- Tian YA, Gao B, Silvera-Batista C et al (2010) Transport of engineered nanoparticles in saturated porous media. *J Nanopart Res* 7:2371–2380
- US EPA (2007) Nanotechnology whitepaper (EPA 100/b-07/001)